Author Manuscript

Author Manuscript

Author Manuscript

Author Manuscript

HHS Public Access

Author manuscript

Oncogene. Author manuscript; available in PMC 2017 May 21.

Published in final edited form as:

Oncogene. 2017 April 20; 36(16): 2215–2227. doi:10.1038/onc.2016.389.

Wwox-Brca1 interaction: Role in DNA repair pathway choice

Morgan S. Schrock[1], **Bahadir Batar**[#1], **Jaeho Lee**[#2], **Teresa Druck**[1], **Brent Ferguson**[2], **Ju Hwan Cho**[3], **Kenneth Akakpo**[1], **Hoda Hagrass**[1,#], **Nyla A. Heerema**[4], **Fen Xia**[3,+], **Jeffrey D. Parvin**[5], **C. Marcelo Aldaz**[2,^], and **Kay Huebner**[1,^]

[1]Department of Cancer Biology and Genetics and Comprehensive Cancer Center, The Ohio State University Wexner Medical Center Columbus, OH 43210

[2]Department of Epigenetics and Molecular Carcinogenesis, Science Park, The University of Texas MD Anderson Cancer Center, Smithville, TX 78957

[3]Department of Radiation Oncology and Comprehensive Cancer Center, The Ohio State University Wexner Medical Center Columbus, OH 43210

[4]Department of Pathology and Comprehensive Cancer Center, The Ohio State University Wexner Medical Center Columbus, OH 43210

[5]Division of Computational Biology & Bioinformatics, Department of Biomedical Informatics and Comprehensive Cancer Center, The Ohio State University Wexner Medical Center, Columbus, OH 43210

[#] These authors contributed equally to this work.

Abstract

In this study, loss of expression of the fragile site encoded Wwox protein, was found to contribute to radiation and cisplatin resistance of cells, responses that could be associated with cancer recurrence and poor outcome. *WWOX* gene deletions occur in a variety of human cancer types and reduced Wwox protein expression can be detected early during cancer development. We find that Wwox loss is followed by mild chromosome instability in genomes of mouse embryo fibroblast cells from Wwox knockout mice. Human and mouse cells deficient for Wwox also exhibit significantly enhanced survival of ionizing radiation and bleomycin treatment, agents that induce double-strand breaks (DSBs). Cancer cells that survive radiation recur more rapidly in a xenograft model of irradiated breast cancer cells; Wwox-deficient cells exhibited significantly shorter tumor latencies *vs* Wwox-expressing cells. This Wwox effect has important consequences in human disease: in a cohort of cancer patients treated with radiation, Wwox-deficiency significantly correlated with shorter overall survival times. In examining mechanisms underlying

Users may view, print, copy, and download text and data-mine the content in such documents, for the purposes of academic research, subject always to the full Conditions of use:http://www.nature.com/authors/editorial_policies/license.html#terms

[^]Correspondence: Kay Huebner, PhD, Department of Cancer Biology and Genetics, the Ohio State University Comprehensive Cancer Center, Biomedical Research Tower Room 916, 460 W 12th Avenue, Columbus, OH 43210; ph (614) 292-4850, fax (614) 688-8675, kay.huebner@osumc.edu; C. Marcelo Aldaz, MD, PhD, The University of Texas MD Anderson Cancer Center, Science Park, 1808 Park Road 1C, Smithville, TX 78957. ph: (512) 237-9530; fax: (512) 237-2475; maaldaz@mdanderson.org.

[#]current addresses: Hoda Hagrass, Asst Prof, Zagazig University, Zagazig, Egypt, currently visiting Asst Prof, United Arab Emirates

[+]Department of Radiation Oncology, University of Arkansas for Medical Sciences, Little Rock, Arkansas, USA

CONFLICT OF INTEREST All authors declare no conflict of interest.

Supplementary information accompanies the paper on the *Oncogene* website (http://www.nature.com/onc).

Author Manuscript Author Manuscript Author Manuscript Author Manuscript

Wwox-dependent survival differences, we found that Wwox-deficient cells exhibit enhanced homology directed repair (HDR), and decreased non-homologous end-joining repair, suggesting that Wwox contributes to DNA DSB repair pathway choice. Upon silencing of Rad51, a protein critical for HDR, Wwox-deficient cells were resensitized to radiation. We also demonstrated interaction of Wwox with Brca1, a driver of HDR, and show *via* immunofluorescent detection of repair proteins at ionizing radiation-induced DNA damage foci that Wwox expression suppresses DSB repair at the end-resection step of HDR. We propose a genome caretaker function for Wwox, in which Brca1-Wwox interaction supports non-homologous end-joining as the dominant DSB repair pathway in Wwox-sufficient cells. Together, the experimental results suggest that reduced Wwox expression, a common occurrence in cancers, dysregulates DSB repair, enhancing efficiency of likely mutagenic repair, and enabling radiation and cisplatin treatment resistance.

Keywords

DNA double-strand breaks; radiation resistance; genome caretaker; common fragile site FRA16D

INTRODUCTION

The FRA16D locus at 16q23 is a common fragile site (CFS) that forms gaps or breaks upon replication stress and is altered in many human cancers, showing up to 52% loss of heterozygosity in breast tumors[1]. The 1.2 Mb *WWOX* gene is located within this fragile region[2], and reduced Wwox protein expression has been correlated with breast cancer progression and poor prognosis[1]. Mouse models confirm a tumor suppressor function for Wwox, as complete knockout mice on various genetic backgrounds was postnatal lethal[1,3]. In addition, Wwox haploinsufficient mice, with a mammary tumor-susceptible C3H background, exhibit increased mammary gland tumorigenicity[4] and re-expression of Wwox decreases tumor burden in ovarian and breast cancer xenografts[5,6].

Recently, FRA16D has been identified as the most active CFS in epithelial cells[7] and large cancer copy number alteration studies identified *WWOX* as the third most commonly deleted gene across human cancers[8,9]. Despite many lines of evidence that suggest a role for loss of Wwox in the progression of cancer[10], our understanding of Wwox tumor suppressive function is incomplete. Wwox protein exhibits distinct structural domains, two adjacent N terminal WW protein-binding domains and a short-chain dehydrogenase/reductase (SDR) domain in its central region believed to play a role in steroid hormone metabolism[2,11] and cellular respiration[12]. The first WW domain binds proteins with a PPxY or PPxL motif and many interactors have been identified, including p73, Ap2γ, ErbB-4, Smad3, and ATM[5,13–16], associated with induction of apoptosis, regulation of proliferation, interaction with extracellular matrix and checkpoint activation. Wwox functional interaction with these proteins has provided thus far the main clues for the role of Wwox in the prevention of cancer development.

In this study, we further examined the role of Wwox-deficiency in cancer progression, specifically in the context of DNA damage. Our initial observation that Wwox ko mouse embryonic fibroblasts (MEFs) showed increased allele copy number gains and losses relative

Author Manuscript Author Manuscript Author Manuscript Author Manuscript

to wt MEFs led us to hypothesize that Wwox protein exhibits a genome caretaker function, suppressing mutations. We show that loss of Wwox expression significantly alters usage of all four DSB repair pathways, suggesting a role for Wwox in pathway choice. Enhanced HDR in Wwox-deficient cells permits significantly increased resistance to cisplatin and radiation treatment associated cell killing, a finding with clinical implications. Finally, we delineate a caretaker function for Wwox in DSB repair pathway choice, and propose its dependence on interaction with Brca1 protein.

RESULTS

Wwox ko MEFs exhibit chromosomal alterations and shared CNVs

To determine if Wwox contributes to genome stability, karyotype and copy number variation (CNV) analyses were carried out using Wwox ko and wt MEF cell lines. Karyotype analysis of three cell lines (two ko and one wt, established from Wwox ko mouse models described previously[3,17]) showed near tetraploidy with chromosomal losses and gains (Supplementary Figure 1). Both ko MEFs, exhibited two structural abnormalities not present in the wt cell line: del(7)(A1B4) and del(4)(C4). Loss of the distal arm of chromosome 4 encompasses the murine *Cdkn2a* gene, encoding p16, a locus frequently deleted in human cancers and in cultured cells[18]. Hemizygous del(7)A1B4 encompasses 48.5 Mb and >650 genes.

CNVs, defined as allele gains or losses spanning >10 kb in size, were assessed in DNAs of MEFs from two distinct Wwox ko mouse models and compared to DNAs from corresponding wt littermates (cell line pairs, KO5/WT4 from Wwox ko[17] and Wwox5/Wwox3 from a different Wwox ko mouse model[3]). CNVs were detected through array comparative genomic hybridization (aCGH). Three distinct deletions were shared by the two ko MEF lines at chromosome locations 1H6, 4B3 and 8C2 (Tables 1a, 1b).

The karyotype and CNV results suggest that absence of Wwox protein is associated with mild genome instability, likely stemming from endogenous DNA damage, prompting our hypothesis that Wwox participates in protecting the genome from damage. We first considered whether Wwox loss leads to un-induced genome damage (i.e., damage not due to exposure to exogenous cytotoxic agent), but comet assay, which detects DNA double-strand breaks (DSBs) as comet tails, and immunofluorescence assays for DSB markers, 53BP1 and γH2AX, did not reveal differences in untreated Wwox-deficient and expressing cells (Supplementary Figure 2).

Wwox-deficient cells exhibit increased survival of ionizing radiation-induced DSBs

To determine if Wwox expression may affect repair of induced DSBs, we investigated the effects of ionizing radiation (IR) on various Wwox-deficient *vs* sufficient cells. Early passage MEFs were exposed to increasing IR doses up to 10 Gy, and plated for clonogenicity to quantify cell survival and proliferation. We observed a significant difference ($P<0.01$) in survival at doses 7.7 Gy and higher (Figure 1a), with ko lines KO3 and KO5 surviving 10-fold better than wt cell lines WT4 and WT7. Similarly, survival curves for transformed breast epithelial cell line, MCF10A clones stably transduced with Wwox silencing shRNAs, shWWOXA and shWWOXB[15], demonstrated increased survival at 7.7

Author Manuscript Author Manuscript Author Manuscript Author Manuscript

Gy and above ($P<0.05$) *vs* the Wwox-sufficient Scr RNA transfected cells (Figure 1b). To determine if Wwox loss has a similar effect in cancer cells, we used MDA MB-231 breast adenocarcinoma cells lacking endogenous Wwox expression, which had been stably transduced with a doxycycline inducible Wwox expression vector[15]. Wwox-induced cells that were treated with doxycycline for 24 hrs and were positive for Wwox are denoted as 231/Wwox-pos throughout the manuscript while these Wwox-deficient cells, untreated with doxycycline are referred to as 231/Wwox-neg. Clonogenicity assays of these cells showed that induced Wwox-expression led to reduced survival at 5.1 Gy (Figure 1c, $P<0.05$), the highest dose at which 231/Wwox-pos cells formed colonies. The shWWOXA and shWWOXB cells were also treated with the radiomimetic, bleomycin, a glycopeptide antitumor antibiotic that induces DSBs, and strikingly significant differences in survival were observed; the Wwox-silenced cells survived bleomycin treatments 25-fold better at 1 and 1.5 μg/ml bleomycin and 100-fold better than Wwox-expressing MCF10A cells at 3 μg/ml bleomycin ($P<0.01$) (Figure 1d). To confirm that enhanced survival was due to absence of Wwox, we established clones KO3A and KO5F from the knockout MEF cell lines KO3 and KO5, which were doxycycline-inducible for expression of Wwox. Upon Wwox induction, both clones exhibited significantly decreased survival ($P<0.05$) at 7.7 Gy and higher (Figure 1e, 1f), confirming that Wwox expression sensitizes cells to radiation.

Wwox expression inhibits growth of irradiated cancer cells in vivo

To determine if the IR resistance of Wwox-deficient cells persists *in vivo*, Wwox-induced (231/Wwox-pos) and Wwox-deficient (231/Wwox-neg) breast cancer cells were tested for tumor growth in immunocompromised mice. The rationale was that despite irradiating the same number of cells for the two groups, more 231/Wwox-neg cells would survive IR, forming tumors more quickly than 231/Wwox-pos cells (Figure 2a). Both groups of cells were exposed to 5 Gy IR, immediately harvested and injected (1×10^7 cells/mouse) subcutaneously into the flanks of athymic nude mice. Control mice from each group were unexposed to IR and exhibited mean tumor latencies (days from injection to first sign of tumor) that were not different: 11 days for 231/Wwox-neg cells, 14 days for 231/Wwox-pos cells. For mice receiving irradiated cells, 7/8 mice injected with 231/Wwox-neg cells formed tumors, while 6/8 mice injected with 231/Wwox-pos cells formed tumors. Of the tumor-bearing mice, those injected with 231/Wwox-neg cells had significantly shorter tumor latencies (mean 17 days) *vs* mice receiving 231/Wwox-pos cells (mean 28 days) (Figure 2b) ($P<0.05$).

Next, we sought a human cancer database with expression and clinical data for cancers treated with radiation to determine if loss of Wwox enabled tumor cell resistance to radiation and decreased overall patient survival in a human model. Since we did not find publicly available breast cancer databases with sufficient clinical data or patients treated with radiation, we examined brain cancers *via* The Repository of Molecular Brain Neoplasia Data (REMBRANDT)[19]. Stratification of patients by Wwox expression did not predict overall survival in a large cohort of brain cancer patients (Figure 3c); however, in cancers treated with radiation, reduced Wwox expression correlated significantly with decreased overall survival *vs* Wwox normal cancers (Figure 3d), suggesting that loss of Wwox facilitates resistance to radiation therapy, disease recurrence and shorter overall survival.

Author Manuscript Author Manuscript Author Manuscript Author Manuscript

Collectively, results of the xenograft model and the brain cancer assessment confirm that Wwox loss supports radiation resistance *in vivo* and that Wwox-deficiency provides a survival advantage to cancer cells carrying DSBs.

Wwox expression regulates DSB repair pathway choice

To elucidate the mechanism that underlies Wwox-deficiency associated radiation resistance, we hypothesized that loss of Wwox could enhance DSB repair. Although there are four DSB repair pathways, two pathways predominate: non-homologous end joining (NHEJ), which bluntly re-ligates DSB ends independent of sequence homology, or homology-directed repair (HDR) which prevails in S and G2 cell cycle phases and uses sister chromatids as templates for accurate DSB repair[20]. To assess the HDR pathway in the presence or absence of Wwox, we used the DR-GFP reporter construct[21] that has been stably integrated into HeLa cells[22] and U87 cells[23]. Repair of the DR-GFP construct *via* HDR is measured as the fraction of GFP positive cells. Wwox-sufficient U87 cells transfected with siWwox and I-SceI revealed a 2.5-fold increase in HDR ($P<0.01$) *vs* control cells transfected with siCtrl and I-SceI (Figure 3a). To confirm Wwox specificity, we performed a rescue experiment in the U87 DR-GFP cells by transfecting siWwox (directed toward Wwox 5' UTR) simultaneously with a full-length Wwox expression plasmid, myc-Wwox[13]. When Wwox expression levels were restored in presence of siWwox, we observed decreased HDR, similar to HDR efficiency of Wwox-sufficient cells (Figure 3a). As further confirmation that Wwox deficiency increases HDR efficiency, transfection of endogenous Wwox-deficient HeLa DR-GFP cells with myc-Wwox resulted in a significant decrease ($P<0.05$) in HDR (Figure 3b). Thus, the DR-GFP assays consistently showed that Wwox expression suppressed HDR.

Since HDR and NHEJ have both been implicated in resistance to radiation[24,25], we next assessed the contribution of Wwox to NHEJ efficiency using 293/HW1 cells. Following induction of DSBs and silencing of Wwox, NHEJ is measured by real time PCR using a probe that spans the junction of the break sites[26]. In 293/HW1 cells, silencing Wwox significantly decreased NHEJ by 50% ($P<0.05$) (Figure 3c), indicating that, unlike HDR, Wwox expression enhanced NHEJ.

Since Wwox expression significantly altered the efficiencies of the predominant DSB repair pathways HDR and NHEJ, we also sought to determine the consequences of Wwox loss on the less common, more error-prone pathways: alternative non-homologous end joining (Alt-NHEJ) and single-strand annealing (SSA). Both are mutagenic and result in deletions initiated by 5' to 3' resection from the DSB site up to microhomologous regions[27]. Alt-NHEJ efficiency was assessed in H1299 EJ2 cells[28] *via* restoration of GFP fluorescence following I-SceI transfection. We observed a dramatic, statistically significant ($P<0.0001$) decrease in Alt-NHEJ (Figure 3d) upon transfection with siWwox and I-SceI. This effect was confirmed in a rescue experiment where siWwox and myc-Wwox simultaneously co-transfected with I-SceI restored Wwox expression and significantly increased Alt-NHEJ ($P<0.001$), indicating that Wwox expression significantly enhanced Alt-NHEJ. To evaluate the effects of Wwox on SSA repair, Wwox-deficient HeLa Sa26 cells[29] were transfected with I-SceI plus either empty vector or myc-Wwox (Figure 3e) and % GFP positive cells were assessed. Upon

Author Manuscript Author Manuscript Author Manuscript Author Manuscript

Wwox expression, SSA in HeLa Sa26 cells was dramatically repressed ($P<0.01$) to less than one third, demonstrating that Wwox expression significantly repressed SSA. Altogether the data indicate that Wwox expression significantly alters repair efficiency for all four DSB repair pathways (summarized in Figure 3f) such that Wwox expression enhances NHEJ and Alt-NHEJ, but impairs HDR and SSA.

Enhanced HDR in Wwox-deficient cells results in resistance to radiation and cisplatin

While HDR and SSA repair are both elevated in Wwox-deficient cells, we hypothesized that HDR was responsible for the observed radiation resistance. To verify that Wwox-deficient cells survive IR-induced DSBs due to enhanced HDR, we inhibited HDR *via* transient knockdown of Rad51, a critical protein for HDR-specific strand invasion. As expected, ko MEFs transfected with siCtrl RNAs (solid lines, Figure 3g) exhibited significantly increased survival ($P<0.001$) than wt MEFs, but following Rad51 depletion (dashed lines), ko MEFs had survival curves similar to wt cells. Thus, HDR inhibition significantly decreased survival after radiation ($P<0.001$) only for Wwox ko MEFs, confirming that increased HDR underlies the radiation resistance of Wwox-deficient cells.

Since alterations in DSB repair pathway efficiencies would affect responses to DNA damaging chemotherapeutic agents, we next investigated the effect of Wwox expression on sensitivity to cisplatin, a crosslinking chemotherapeutic agent that causes DSBs. We hypothesized that Wwox-deficient cells would be more resistant to cisplatin *vs* Wwox-sufficient cells because their enhanced HDR would resolve DSBs induced by cisplatin more efficiently. Indeed, treatment of 231/Wwox-neg cells with various doses of cisplatin revealed enhanced survival to cisplatin treatment at 10 μM in 231/Wwox-neg *vs* 231/Wwox-pos cells ($P<0.01$) and at higher doses (Figure 3h). Likewise, ko MEFs survive cisplatin at 25 μM ($P<0.001$) and higher concentrations *vs* WT4 MEF (Figure 3i). Thus, the dysregulation of DSB repair pathways and subsequent enhanced HDR associated with Wwox-deficiency results in cellular resistance to the commonly used breast cancer therapeutic agents: radiation and cisplatin. Given that cellular loss of Wwox encourages therapy resistance, we next sought clues to the mechanism involved in Wwox protein suppression of HDR.

Cell cycle phase distribution in IR-treated Wwox positive and negative cells

Since HDR is thought to occur mainly in S and G2 phases of the cell cycle where a sister chromatid is available as repair template[20], we considered whether cell cycle phase distribution and checkpoint activation differences might contribute to increased HDR and radiation resistance in Wwox-deficient cells. Flow cytometric analysis in 231/Wwox cells, regardless of induced Wwox expression, showed nearly identical cell cycle phase distributions (Figure 4a), with accumulation in G2/M by 10 hrs post-irradiation (Figure 4b), though 231/Wwox-neg cells appeared to have stronger activation of pChk2 and pChk1 (Supplementary Figure 3). Similar experiments in early passage (~p10) Wwox ko and wt MEFs revealed differences for the wt and ko cells in cell cycle phase distribution (Figure 4c) and checkpoint activation (Figure 4d), neither of which activities showed correlation with the responses of the cells to IR (Supplementary Figure 4). Results of the cell cycle analyses of MEFs and 231/Wwox cells demonstrated that the differences in cell cycle kinetics among

Author Manuscript Author Manuscript Author Manuscript Author Manuscript

various Wwox positive and negative cells did not account for the differences in responses to IR exposure.

Brca1 and Wwox proteins form a complex

Given the multiple protein interactors for Wwox, we hypothesized that Wwox interaction with a protein(s) in the HDR pathway might underlie its role in DSB repair pathway choice. Brca1 was a candidate interactor as it contains a PPxL Wwox-binding motif at aa 981 and promotes HDR over NHEJ repair by initiating DSB end resection[30]. To investigate a potential interaction between Wwox and Brca1, we performed GST pull-down experiments using GST fused to various Wwox constructs in HEK293T cells transfected with HA-Brca1 (Figure 5a). A schematic of the Wwox domains is presented in Figure 5c. GST fused to wildtype full-length Wwox bound HA-Brca1 and was detected by anti-HA antibody (Figure 5a, lane 7). Likewise, GST fused to the WW domain fragment (WW1&2, lane 3) bound HA-Brca1, however, the WW domain fragment with mutated WW1 (W44F/P47A)[31], that renders the binding domain non-functional, did not bind HA-Brca1 (lane 4), suggesting that Wwox interaction with Brca1 occurs through the WW1 domain. In support of this, a WW domain with mutated WW2 (Y85A/P88A in lane 5) pulls down HA-Brca1, indicating that WW2 is not essential for the interaction; finally a GST-fused SDR fragment did not bind HA-Brca1 (lane 6) and does not contain either WW domain.

To confirm the Brca1-Wwox interaction, we transfected HEK293T cells with HA-Brca1 plus full-length, myc-tagged Wwox plasmid (myc-Wwox) and performed immunoprecipitation using anti-HA and detection with anti-Brca1 (Figure 5b). HA-Brca1 pulled down myc-Wwox (detected by anti-Wwox) while IgG immunoprecipitation did not detectably bind either protein.

Next, to determine which Brca1 domain was participating in the Wwox interaction, we transfected five Brca1 mutants, harboring deletions from the N to C terminus (Figure 5d), into MDA MB-231 cells with myc-Wwox. The lysates were immunoprecipitated with anti-HA to avoid detecting interactions due to the low level endogenous Brca1 protein expressed in the MB-231 cells. The HA antibody precipitated Wwox in lysates harboring Brca1 deletions at the N, M3 and C regions (lane 6, 9, 10 Figure 5e) but not in lysates expressing Brca1 with the M1 and M2 deleted regions (lane 7, 8 Figure 5e). These interactions were confirmed in the opposite direction, in HEK293T cells transfected with myc-Wwox plus each of the Brca1 deletion mutants (Supplementary Figure 5). Immunoprecipitation using Myc antibody as bait revealed that all Brca1 deletion mutants except M1 and M2 detectably bound myc-Wwox (lanes 6–10, Supplementary Figure 5), suggesting that sequences within the Brca1 aa 305-1292 region are responsible for the Wwox-Brca1 interaction.

Wwox interaction with Brca1 through the WW domain is responsible for decreased survival of DSBs

To confirm whether interaction with Brca1 through the WW domain is responsible for suppression of HDR and sensitivity to DSBs, the MDA MB-231 cells were stably transfected with doxycycline inducible full-length Wwox harboring WW1 mutations[31] W44F/P47A (231/WW1 mut) or full-length Wwox harboring a mutation (Y293F) at the

Author Manuscript Author Manuscript Author Manuscript Author Manuscript

catalytic SDR site (231/SDR mut) and performed clonogenicity assays following increasing doses of IR. These cells are denoted as 231/WW1 mut-pos and 231/SDR mut-pos when treated with doxycycline for 24 hrs and expressing the full length Wwox with WW1 or SDR mutation. Conversely 231/WW1 mut-neg and 231/SDR mut-neg cells express only very low levels of endogenous Wwox. We inferred that if Wwox interaction with Brca1 was critical for suppression of HDR and sensitivity to DSBs, the cells expressing Wwox WW1 mutant would show no difference in IR survival with or without induction, i.e. they would both respond as if Wwox negative, while cells induced to express the Wwox SDR mutant, that maintains a functional WW1 domain, would be IR sensitive. Supplemental Figure 6b demonstrates the inducibility of Wwox expression in these cell lines. As predicted, Figure 5f shows that 231 cells expressing a non-functional WW1 mutant Wwox protein (231/WW1 mut-pos) exhibit an IR survival curve similar to the same cells uninduced for Wwox (231/WW1 mut-neg). This suggests that without a functional WW1 domain, Wwox does not sensitize cells to radiation. Conversely, upon expression of full-length Wwox harboring an SDR mutant, the cells exhibit significantly decreased survival relative to the same cells uninduced (Figure 5g); i.e. the SDR mutant Wwox-expressing cells are sensitive to radiation because they retain a WW1 domain, which interacts with Brca1.

Loss of Wwox expression leads to significant increases in radiation-induced nuclear Rpa32 and Rad51 foci

Since Brca1 forms complexes comprised of varying interacting proteins and these complexes have distinct functions during DSB recognition and repair, we sought to understand how Wwox-Brca1 might enhance NHEJ and suppress HDR, through immunofluorescent detection of critical DSB repair-associated proteins: γH2AX, 53BP1, RIF1, Brca1, Rad51 and Rpa32 (Figure 6). These proteins form foci at DSBs upon irradiation and are involved in DSB recognition, repair pathway choice, and end-resection (Figure 7a, b). Briefly, γH2AX detects DSBs and recruits 53BP1/RIF1 complex, which protects DSB ends and promotes NHEJ. However in S phase, Brca1 is abundant and complexes with the endonuclease CtIP, displaces 53BP1/RIF1 and promotes end-resection through interaction with the MRN complex composed of Mre11, Rad50 and Nbs1. DSB end-resection commits cells to HDR or SSA. The resulting single stranded DNA (ssDNA) is coated with RPA and subsequent formation of Rad51 nucleofilament initiates strand invasion for HDR.

To quantify the accumulation of repair proteins at DSBs, number of positive foci per nucleus were determined in 231/Wwox-pos and 231/Wwox-neg cells following 10 Gy IR as indicated in Figure 6. We observed a statistically significant increase in γH2AX foci at 3 hrs after IR in 231/Wwox-neg cells compared to 231/Wwox-pos cells, likely reflecting the more time-consuming repair process associated with HDR *vs* rapid NHEJ. There were no significant differences in foci of RIF1, 53BP1 or Brca1 proteins at 0, 1, 3 and 6 hrs after IR, suggesting that Wwox interaction with Brca1 does not interfere with recruitment of Brca1 to DSBs and displacement of the 53BP1/RIF1 complex. However, Rpa32 and Rad51 showed significantly increased foci in 231/Wwox-neg cells compared to 231/Wwox-pos cells 1 hr after IR. Increased Rpa32 foci indicate that 231/Wwox-neg cells exhibit enhanced DSB end-

Author Manuscript Author Manuscript Author Manuscript Author Manuscript

resection, therefore we hypothesize that Wwox interaction with Brca1 suppresses DSB end-resection in Wwox-sufficient cells, ultimately promoting NHEJ over HDR.

DISCUSSION

We have established a role for Wwox in regulation of DSB repair, such that Wwox-deficient cells exhibit enhanced HDR and survival of DSB-inducing agents. We also reveal a novel interaction of Wwox protein with Brca1, the genome caretaker that mediates HDR repair of DSBs, and hypothesize that Wwox suppresses HDR through its interaction with Brca1, tipping the pathway choice to NHEJ repair. Unlike a recently reported interaction between Wwox and the kinase, ATM[16], the interaction of Wwox with Brca1 appears not to be dependent on DNA damage. Our co-immunoprecipitation experiments confirmed that Wwox may interact with Brca1 near the ^{981}PPLF^{984} motif since Brca1 mutants lacking aa 305-1292 did not bind Wwox. Therefore, we propose that in Wwox-sufficient cells, Wwox binds Brca1, directly or indirectly, along this central region, competing with other Brca1-interacting proteins critical for promoting HDR. One candidate, Rad50, a component of the MRN complex, binds Brca1 at aa 341–758[32]. This interaction is responsible for stimulating nuclease activity of CtIP and MRN to enable end-resection, which commits cells to HDR or SSA. We offer a model (Figure 7c) that proposes Wwox competes with Rad50 for binding to Brca1 and subsequently impairs endresection in Wwox-sufficient cells. In this way, Wwox-deficiency, which commonly occurs in cancer cells, lacks an inhibitory regulatory step, resulting in enhanced end-resection and HDR repair, ultimately enabling the cells to survive DNA damage-inducing cytotoxic treatments.

With this delineation of a role for Wwox in DNA repair pathway choice, we have established that Wwox is a genome caretaker, apparently paradoxically, through its role in supporting NHEJ repair, an imperfect pathway. If Wwox is involved in genome caretaking how can it be that absence of Wwox pushes cells toward HDR, the presumptive pathway-of-choice for best repair, and in this case, the pathway to increased survival cellular survival of severe induced DNA damage? We believe that the enhancement of HDR due to Wwox absence is mutagenic in Wwox-deficient cells based on the cell cycle analysis data (Figure 4), which demonstrates that Wwox expression does not affect cell cycle phase. This implies that although HDR is enhanced, it is not restricted to S or G2 phases of the cell cycle in Wwox-deficient cells. If HDR should occur in the G1 phase, when sister chromatids are unavailable, the homology search may take place across the entire genome, increasing opportunities for mutagenesis due to inappropriate pairing[33]. In addition, we have shown that loss of Wwox significantly alters the efficiencies of the remaining DSB repair pathways (summarized in Figure 3f), impairing NHEJ and Alt-NHEJ, but enhancing SSA, a mutagenic repair pathway that typically generates large deletions with no insertions[27]. Since the DSB repair pathways are complex and interconnected, it is difficult at this point to specifically assign the mutational burden or consequences of Wwox dysregulation to individual altered repair pathways following DNA damage. However, the chromosomal instability and large deletions observed through karyotype and CNV analysis associated with Wwox loss supports the idea that Wwox-deficiency is mutagenic. Since loss of Wwox has been well documented in association with the progression of numerous human cancers cancers[1,10], we

Author Manuscript Author Manuscript Author Manuscript Author Manuscript

propose that long-term, Wwox-deficient cells carry a higher mutational burden despite short-term cellular survival of DNA DSBs due to enhanced HDR.

Our findings have important, broad therapeutic implications as Wwox is among the most commonly deleted genes in a wide variety of common human cancers[1,8,9,34]. We propose that determining Wwox expression levels could be an important predictor of response to radiation, cisplatin and possibly other chemotherapeutic agents. Stratifying cancers by Wwox expression could allow physicians to determine whether particular cancers would be good candidates for radiation and perhaps also inform the dosage of DSB-inducing treatments. Most importantly, we show that selectively inhibiting the HDR pathway in Wwox-deficient cells abolishes their radio-resistance and re-sensitizes them to radiation, suggesting the use of HDR inhibitors in conjunction with radiation for treatment of Wwox-deficient tumors.

MATERIALS AND METHODS

Ethics statement and Xenograft

Animal experiments were in accordance with the `Guide for the Care and Use of Laboratory Animals' of the National Institutes of Health and The Ohio State University IACUC Protocol 2014A00000017. A total of 10 athymic nude female mice (JAX stock# 007850) were injected at 8 weeks of age with 1×10^7. Positive control mice (n=2) received un-irradiated cells while experimental mice (n=4 for each group) received cells exposed to 5 GY. There were two groups of experimental mice: Group#1 received 231/Wwox-pos cells, and Group#2 received 231/Wwox-neg cells.

Cell lines

MEFs were isolated from individual 13-day embryos of *Wwox*$^{+/+}$ and *Wwox*$^{-/-}$ mixed background (B6 × 129 SvJ) strain pregnant females and designated MEF WT4, WT7, KO3 and KO5 cell lines. They were cultured in DMEM with 10% FBS, 100 μg/ml gentamicin and established as described[35]. Wwox3 (Wwox$^{+/+}$) and Wwox5 (Wwox$^{-/-}$) MEFs have been described[3]. Breast cancer cell line, MDA MB-231, and Wwox-inducible derivatives were maintained under standard conditions. The MCF10A cell line and Wwox stably silenced clones, shWWOXA and shWWOXB have been previously described[15]. Supplementary Figure 6a and b shows relative Wwox expression of cell lines used throughout the manuscript.

Chemicals and plasmids

MMC (SCBT), Cisplatin (Sigma Aldrich), ABT-888 (SelleckChem, Houston, TX) and Bleomycin (SCBT, Santa Cruz, CA) were purchased in DMSO or prepared as stocks in DMSO. The Brca1 deletion mutants[36] are HA-tagged and correspond to deletions within the Brca1 protein as illustrated in Figure 6d. The Brca1 ΔM3 mutant (aa 1290–1530) was generated from full length HA-Brca1 plasmid[37] using methods described in Gibson Assembly Cloning Kit (New England BioLabs) and primer sequences: BRCA1-305-F: CAGAATGAATGTAGAAAAGGCTG, BRCA1-305-1290-del-Rev: gttgctcctccacatcaacaacACATTTTGTTTCCTCACTAAG, BRCA1-305-1290-del-For:

Author Manuscript Author Manuscript Author Manuscript Author Manuscript

cttagtgaggaaacaaaatgtGTTGTTGATGTGGAGGAGCAAC, pcDNA-Xho-rev: TAGGGCCCTCTAGATGCATGC. XhoI and EcoRI restriction digestion and sequencing validated the correct insertion and sequence. The full length myc-Wwox plasmid[13] and deletion mutants[15] were previously described.

Transient transfections

The MDA MB 231 cell line with doxycycline-inducible Wwox lentiviral-based system was previously described[15] and is referred to as 231/Wwox. For transient knockdowns, mouse MEFs WT4, WT7, KO3, and KO5 were transfected with siRNAs targeting Rad51 or a non-specific control siRNA using standard Dharmacon protocol (Dharmacon, Lafayette, CO).

Clonogenicity

Clonogenicity assays were performed as described[35]. Cells were harvested immediately after exposure to IR and 4 hrs following exposure to MMC, 24 hrs after ABT-888, and 2 hours after bleomycin treatment. Survival (%) was calculated based on plating efficiencies of cells with no exposure to treatment.

DSB repair assays

To assess HDR, two cell lines with DR-GFP stable integrations were used: HeLa cells[22] which are Wwox-deficient and U87 cells[23] which are Wwox-sufficient. The NHEJ experiment was performed in Wwox-sufficient HEK293 cells with stably integrated NHEJ substrate, HW1. HDR, NHEJ, Alt-NHEJ and SSA assays were performed as previously described[22,26]. Wwox-deficient HeLa cells were transfected with 300 ng of myc-Wwox plasmid, empty myc vector, or myc-Wwox + siWwox where the myc-Wwox plasmid is resistant to silencing by the siRNAs. Wwox-sufficient cell lines, U87, HEK293, and H1299 cells were transfected with siWwox or scrambled control siRNAs (Dharmacon).

Immunoblot and co-immunoprecipitation assays

For immunoblot analysis, cells were lysed with RIPA buffer (TFS, Waltham, MS) supplemented with Halt Protease Cocktail Inhibitors (TFS) or when detecting Brca1, lysed with low salt NP40 buffer as described[26]. When transfecting plasmids, ~75–85% confluent cells were overlayed with a mixture containing 2 μg of plasmid DNA, 12 μl Lipofectamine2000 (Invitrogen) in 200 μl Opti-Mem, and medium was changed 4–6 hrs later. Cells were harvested for co-Immunoprecipitation 24 hrs later. Approximately 20 μg of antisera was used in binding of protein baits for co-immunoprecipitation: Brca1[37], Wwox[38], myc[39], HA[40] or HA (Covance, Princeton, NJ), and IgG (SCBT #2025) (Supplementary table 1). GST-pulldown with Wwox wt GST-fusion protein and Wwox derivatives was performed as previously described[31]. The GST-WW domain fragments harbored mutations at W44F + P47A (WW1) and Y85A + P88A (WW2).

Human brain cancer analysis (REMBRANDT)

Brain cancer expression data and patient clinical data were accessed through Georgetown Database of Cancer (https://gdoc.georgetown.edu/gdoc/). Two patient groups were created: group 1, detailed in Supplementary Tbl2 and depicted in Figure 2c was made up of all brain

Author Manuscript Author Manuscript Author Manuscript Author Manuscript

cancer patients that had both clinical data and expression data, while group 2, detailed in Supplementary Tbl3 and depicted in Figure 2d, was composed of patients from group 1 that were treated with radiation. Kaplan Meier plots were generated through the KM Clinical Plot application, a fold change of 2 was used to designate patients as down-regulated Wwox expression.

Supplementary Material

Refer to Web version on PubMed Central for supplementary material.

ACKNOWLEDGEMENTS

Support was by Pelotonia Graduate and Post-Doctoral Fellowships (MS, BB), 9T32OD010429 (MS), CA154200 (KH), R01CA120516 (KH), NIH/NCI R01 CA102444 (CMA), CA198228 (JP), a fellowship from The Scientific and Technological Research Council of Turkey (TUBITAK to BB), and a graduate research scholarship from the Egyptian Cultural and Educational Bureau (to HH). We thank the OSU CMIF shared Facility for confocal microscopy and the Genome Quebec company for assistance with CNA experiments. We thank Matthew Guggenbiller (OSUMC) for help with the analysis of the brain cancer cohort and Megan Lowery and Richard D. Wood (The University of Texas MD Anderson Cancer Center, Smithville, TX) for providing the data in Figure 1d and Jenna Karras and T. Banerjee for helpful discussions. We are especially appreciative of the additional funding by the breast cancer support foundations, The Stefanie Spielman Fund of the OSUCCC and The Anne M. Wolfe Foundation (Anne's Army).

REFERENCES

1. Aldaz CM, Ferguson BW, Abba MC. WWOX at the crossroads of cancer, metabolic syndrome related traits and CNS pathologies. Biochim Biophys Acta. 2014; 1:188–200.
2. Bednarek AJ, Laflin KJ, Daniel RL, Liao Q, Hawkins KA, Aldaz CM. WWOX, a novel WW domain-containing proteins mapping to human chromosome 16q23.3–16q24.1, a region frequently affected in breast cancer. Can Res. 2000; 60:2140–2145.
3. Aqeilan RI, Trapasso F, Hussain S, Costinean S, Marshall D, Pekarsky Y, et al. Targeted deletion of Wwox reveals a tumor suppressor function. Proc Natl Acad Sci. 2007; 10:3949–54.
4. Abdeen SK, Salah Z, Maly B, Smith Y, Tufail R, Abu-Odeh M, Zanesi N, Croce CM, Nawaz Z, Aqeilan RI. Wwox inactivation enhances mammary tumorigenesis. Oncogene. 2011; 36:3900–6.
5. Aqeilan RI, Donati V, Palamarchuk A, Trapasso F, Kaou M, Pekarsky Y, et al. WW domain-containing proteins, WWOX and YAP, compete for interaction with ErbB-4 and modulate its transcriptional function. Cancer Res. 2005; 15:6764–72.
6. Iliopoulos D, Fabbri M, Druck T, Qin HR, Han SY, Huebner K. Inhibition of breast cancer cell growth in vitro and in vivo: effect of restoration of Wwox expression. Clin *Cancer Res*. 2007; 13:268–74. [PubMed: 17200365]
7. Letessier A, Millot GA, Koundrioukoff S, Lachages A, Vogt N, Hansen RS, et al. Cell-type-specific replication initiation programs set fragility of the FRA3B fragile site. Nature. 2011; 470:120–123. [PubMed: 21258320]
8. Bignell GR, Greenman CD, Davies H, Butler AP, Edkins S, Andrews JM, et al. Signatures of mutation and selection in the cancer genome. Nature. 2010; 463:893–898. [PubMed: 20164919]
9. Beroukhim R, Mermel CH, Porter D, Wei G, Raychaudhuri S, Donovan J, et al. The landscape of somatic copy-number alteration across human cancers. *Nat*ure. 2010; 18:899–905.
10. Salah Z, Aqeilan R, Huebner K. WWOX gene and gene product: tumor suppression through specific protein interactions. Future Oncol. 2010; 2:249–259.
11. Aqeilan RI, Hagan JP, de Bruin A, Rawahneh M, Salah Z, Gaudio E, et al. Targeted ablation of the WW domain-containing oxidoreductase tumor suppressor leads to impaired steroidogenesis. Endocrinol. 2009; 3:1530–1535.

Author Manuscript Author Manuscript Author Manuscript Author Manuscript

12. Choo A, O'Keefe LV, Lee CS, Gregory SL, Shaukat Z, Colella A, Lee K, Denton D, Richards RI. Tumor suppressor WWOX moderates the mitochondrial respiratory complex. Genes Chrom Cancer. 2015; 54:745–61. [PubMed: 26390919]
13. Aqeilan RI, Pekarsky Y, Herrero JJ, Palamarchuk A, Letofsky J, Druck T, et al. Functional association between Wwox tumor suppressor protein and p73, a p53 homolog. Proc Natl Acad Sci. 2004; 101:4401–4406. [PubMed: 15070730]
14. Aqeilan RI, Palamarchuk A, Weigel RJ, Herrero JJ, Pekarsky Y, Croce CM. Physical and functional interactions between the Wwox tumor suppressor protein and the Ap-2γ transcription factor. Cancer Res. 2004; 64:8256–8261. [PubMed: 15548692]
15. Ferguson BW, Gao X, Zelazowski MJ, Lee J, Jeter CR, Abba MC, et al. The cancer gene WWOX behaves as an inhibitor of SMAD3 transcriptional activity via direct binding. BMC Cancer. 2013; 13:593. [PubMed: 24330518]
16. Abu-Odeh M, Salah Z, Herbel C, Hofmann TG, Aqeilan RI. WWOX, the common fragile site FRA16D gene product, regulates ATM activation and the DNA damage response. Proc Natl Acad Sci. 2014; 111:E4716–25. [PubMed: 25331887]
17. Ludes-Meyers JH, Kil H, Parker-Thornburg J, Kusewitt DF, Bedford MT, Aldaz CM. Generation and characterization of mice carrying a conditional allele of the Wwox tumor suppressor gene. PLoS One. 2009; 4:e7775. [PubMed: 19936220]
18. Hartmann C, Kluwe L, Lucke M, Westphal M. The rate of homozygous CDKN2A/p16 deletions in glioma cell lines and in primary tumors. Int J Oncol. 1999; 5:975–982.
19. Scarpace, L., Flanders, AE., Jain, R., Mikkelsen, T., Andrews, DW. Data from REMBRANDT. The Cancer Imaging Archive. 2015. http://doi.og/10.7937/K9/TCIA.2015.588OZUZB
20. Driscoll M, Jeggo PA. The role of double-strand break repair-insights from human genetics. Nat Rev Genet. 2006; 7:45–54. [PubMed: 16369571]
21. Pierce AJ, Johnson RD, Thompson LH, Jasin M. XRCC3 promotes homology-directed repair of DNA damage in mammalian cells. Genes Dev. 1999; 13:2633–2638. [PubMed: 10541549]
22. Ransburgh DJ, Chiba N, Ishioka C, Toland AE, Parvin JD. Identification of breast tumor mutations in BRCA1 that abolish its function in homologous DNA recombination. Cancer Res. 2010; 70:988–95. [PubMed: 20103620]
23. Golding SE, Rosenberg E, Khalil A, McEwen A, Holmes M, Neill S, et al. Double strand break repair by homologous recombination is regulated by cell cycle-independent signaling via ATM in human glioma cells. J Biol Chem. 2004; 279:15402–15410. [PubMed: 14744854]
24. Lim YC, Roberts TL, Day BW, Stringer BW, Kozlov S, Fazry S, et al. Increased sensitivity to ionizing radiation by targeting the homologous recombination pathway in glioma initiating cells. Mol Oncol. 2014; 8:1603–1615. [PubMed: 25017126]
25. Li Y, Wang X, Pan Y, Lee D, Chowdhury D, Kimmelman AC. Inhibition of non-homologous end joining repair impairs pancreatic cancer growth and enhances radiation response. PLoS One. 2012; 7:e39588. [PubMed: 22724027]
26. Hu Y, Wang C, Huang K, Xia F, Parvn JD, Mondal N. Regulation of 53BP1 protein stability by RNF8 and RNF168 is important for efficient DNA double-strand break repair. PLoS One. 2014; 9:1–13.
27. Ceccaldi R, Rondinelli B, D'Andrea AD. Repair pathway choices and consequences at the double-strand break. Trends Cell Biol. 2016; 26:52–64. [PubMed: 26437586]
28. Bennardo N, Cheng A, Huang N, Stark JM. Alternative-NHEJ is a mechanistically distinct pathway of mammalian chromosome break repair. PLoS Genet. 2008; 6:e1000110.
29. Towler WI, Zhang J, Ransburgh DJ, Toland AE, Ishioka C, Chiba N, et al. Analysis of BRCA1 variants in double-strand break repair by homologous recombination and single-strand annealing. Hum Mutat. 2013; 3:439–445.
30. Zimmerman M, de Lange T. 53BP1: pro-choice in DNA repair. Trends Cell Biol. 2014; 24:108–117. [PubMed: 24094932]
31. Ludes-Meyers JH, Kil H, Bednarek AK, Drake J, Bedford MT, Aldaz CM. WWOX binds the specific proline-rich ligand PPXY: identification of candidate interacting proteins. Oncogene. 2004; 29:5049–55.
32. Christou CM, Kyriacou K. BRCA1 and its network of interacting proteins. Biol. 2013; 2:40–63.

Author Manuscript Author Manuscript Author Manuscript Author Manuscript

33. Rodgers K, McVey M. Error-prone repair of DNA double-strand breaks. J Cell Physiol. 2015; 231:15–24.
34. Schrock MS, Huebner K. WWOX: a fragile tumor suppressor. *Exp Biol Med* (Maywood). 2015; 240:296–304. [PubMed: 25538133]
35. Miuma S, Saldivar JC, Karras JR, Waters CE, Paisie CA, Wang Y, et al. Fhit deficiency-induced global genome instability promotes mutation and clonal expansion. PLoS One. 2013; 8:e80730. [PubMed: 24244712]
36. You F, Chiba N, Ishioka C, Parvin JD. Expression of an amino-terminal BRCA1 deletion mutant causes a dominant growth inhibition in MCF10A cells. Oncogene. 2004; 23:5792–8. [PubMed: 15122325]
37. Sankaran S, Starita LM, Simons AM, Parvin JD. Identification of domains of BRCA1 critical for the ubiquitin-dependent inhibition of centrosome function. Cancer Res. 2006; 8:4100–4107.
38. Guler G, Uner A, Guler N, Han S, Iliopoulos BS, Hauck WW, et al. The fragile genes FHIT and WWOX are inactivated coordinately in invasive breast carcinoma. Cancer. 2004; 100:1605–1614. [PubMed: 15073846]
39. Veronese A, Visone R, Consiglio J, Acunzo M, Lupini L, Kim T, et al. Mutated beta-catenin evades a microRNA-dependent regulatory loop. Proc Natl Acad Sci. 2011; 12:4840–4845.
40. Huang J, Yan J, Zhang J, Zhu Z, Wang Y, Shi T, et al. SUMO1 modification of PTEN regulates tumorigenesis by controlling its association with the plasma membrane. Nat. Commun. 2012; 3:911. [PubMed: 22713753]
41. Saldivar JC, Miuma S, Bene J, Hosseini SA, Shibata H, Sun J, et al. Initiation of genome instability and preneoplastic processes through loss of Fhit expression. PLoS Genet. 2012; 8:e1003077. [PubMed: 23209436]
42. Hosseini SA, Horton S, Saldivar JC, Miuma S, Stampfer MR, Heerema NA, et al. Common chromosome fragile sites in human and murine epithelial cells and FHIT/FRA3B loss-induced global genome instability. Genes Chrom Cancer. 2013; 52:1017–29. [PubMed: 23929738]

Author Manuscript Author Manuscript Author Manuscript Author Manuscript

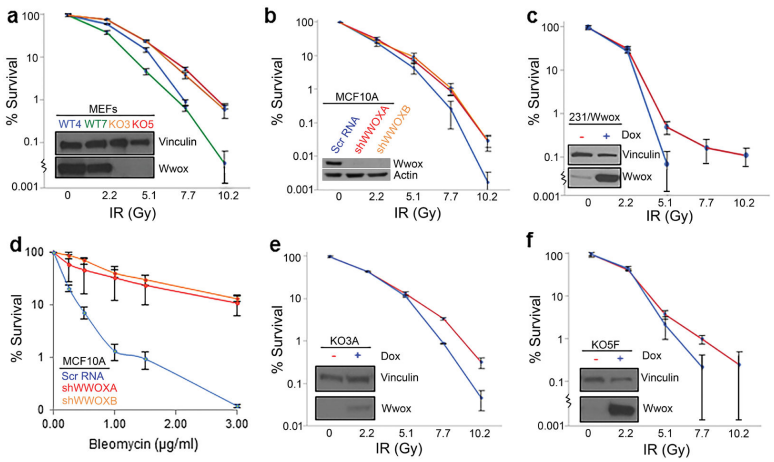

Figure 1.

Human and mouse Wwox-deficient cells exhibit increased survival to DSBs. Wwox-deficient cell lines are represented in red or orange, Wwox-sufficient cell lines are represented in blue or green. (**a**) Graph depicting % survival of MEF cell lines, Wwox ko (KO3, KO5) and wt (WT4, WT7) following IR treatment. (**b**) Graph depicting % survival in the transformed breast epithelial MCF10 cells and Wwox stably silenced MCF10A clones, shWWOXA and shWWOXB, following increasing IR doses. (**c**) Graph depicting % survival in doxycycline-inducible MDA MB-231 cells following IR treatment. (**d**) Graph depicting % survival in MCF10A cells and shWWOXA and shWWOXB clones following Bleomycin treatment; (**e**) Graph depicting % survival of doxycycline-inducible KO3 clone, 2A2, with and without doxycycline after IR treatment. (**f**) Graph depicting % survival of doxycycline-inducible KO5 clone, 2F2, with and without doxycycline after various IR doses. (**a–f**) Embedded Western Blots (WBs) demonstrate Wwox expression in the cell lines. Experiments were performed in triplicate. Error bars denote one standard error; lower standard error bars are abbreviated due to log scale.

Author Manuscript Author Manuscript Author Manuscript Author Manuscript

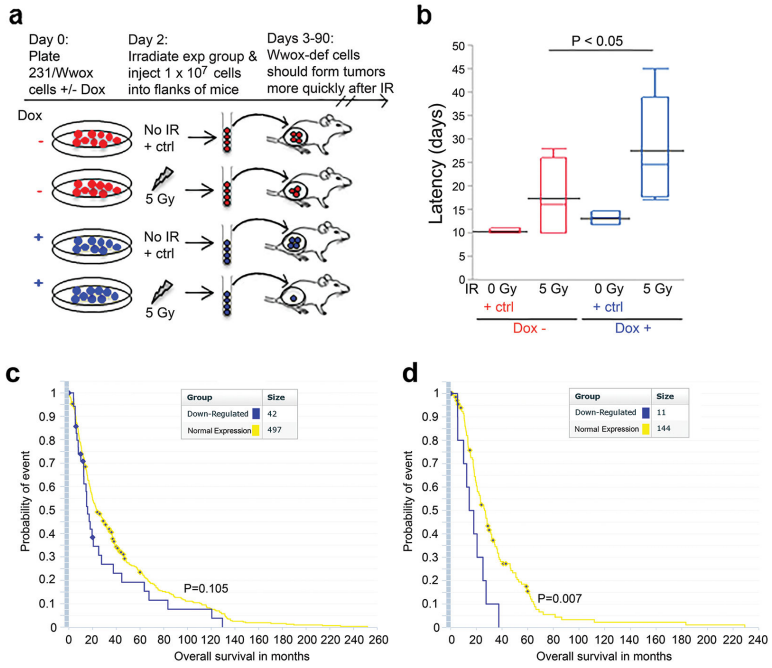

Figure 2.

Wwox expression inhibits growth of irradiated cancer cells *in vivo* in mouse and human models. Wwox-deficient cells are depicted as red, Wwox-sufficient cells are depicted as blue. (**a**) Illustration of experimental rationale: on injection of equal cell numbers, it is expected that more Wwox-deficient cells will survive IR and therefore form earlier tumors. (**b**) Box plot depicting tumor latency (days from injection to sign of first tumor) of mice which developed tumors following injection of Wwox-deficient or Wwox-expressing IR and non-IR treated 231/Wwox cells. Tumors developing in mice injected with 231/Wwox- cells exhibited significantly shorter latencies (P <0.05) following exposure to 5 Gy IR. (**c**) Kaplan Meier plot of all brain cancer patients indicating no significant difference in overall survival (months) of brain cancer patients stratified by Wwox expression. (**d**) Kaplan Meier plot of only brain cancer patients treated with radiation, demonstrating a significantly shorter survival (P<0.01) of Wwox-deficient brain cancer patients compared to Wwox-sufficient brain cancer patients upon treatment with radiation.

Author Manuscript Author Manuscript Author Manuscript Author Manuscript

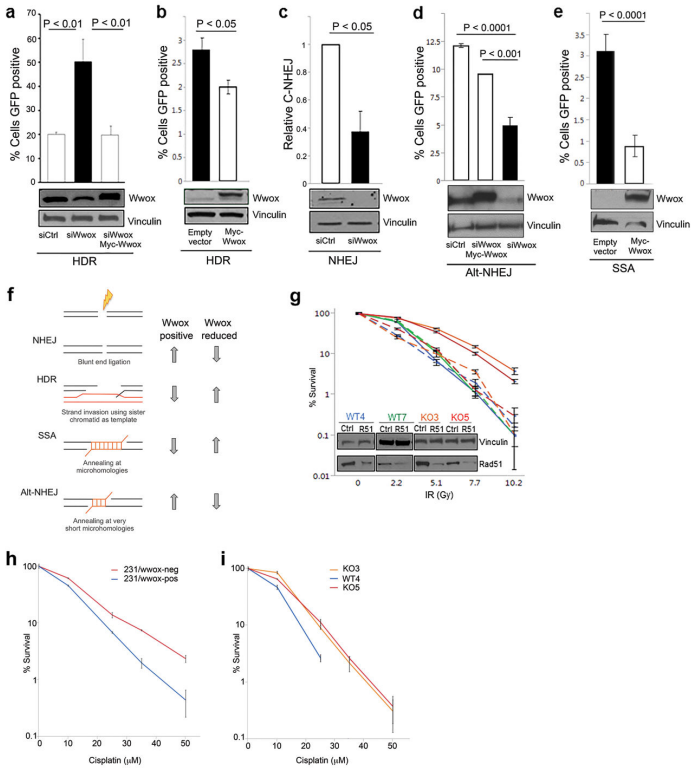

Figure 3.

Wwox-deficient cells exhibit increased homologous recombination, which is responsible for enhanced IR survival. In bar charts, Wwox-deficient cells are depicted as black and Wwox-sufficient cells are depicted as white. WBs below bar charts demonstrate transfection efficiency and Wwox expression. (**a**) Bar graph indicating % of cells positive for GFP as indication of relative HR, with corresponding immunoblots of U87 cells carrying HR reporter, DR-GFP, and transfected with siCtrl, siWwox and siWwox + myc-Wwox plasmid resistant to silencing. (**b**) Graph indicating % GFP positive HeLa cells DR-GFP transfected with empty vector or Myc-Wwox. (**c**) Bar graph indicating relative mRNA as a measure of C-NHEJ in H1299 cells carrying pHW1 and transfected with siCtrl and siWwox. (**d**) Bar graph depicting fraction of GFP positive cells in H1299 EJ2 cells indicating relative Alt-NHEJ efficiencies following transfection with siCtrl, siWwox + myc-Wwox, and siWwox. (**e**) Bar graph indicating % of GFP positive cells as a measure of SSA in HeLA Sa26 cells following transfection with empty vector and myc-Wwox. (**f**) Schematic of the four DSB repair pathways: NHEJ, HDR, SSA, and Alt-NHEJ and corresponding changes in efficiency dependent on Wwox expression (right). (**g**) Line graph indicating % survival of MEFs with and without Rad51 silencing (denoted as R51 in embedded WBs) following exposure to designated IR doses. Solid lines indicate survival of MEFs with normal Rad51 expression while dashed lines indicate Rad51 silenced cells. (**h**) Line graph depicting % survival of 231/Wwox cells with and without doxycycline following exposure to various levels of cisplatin for two hours. (**i**) Line graph depicting % survival of MEFs following exposure to various levels of cisplatin for two hrs. (**a–e, g–i**) Data from three independent experiments were subjected to two-tailed Student's t-test.

Author Manuscript Author Manuscript Author Manuscript Author Manuscript

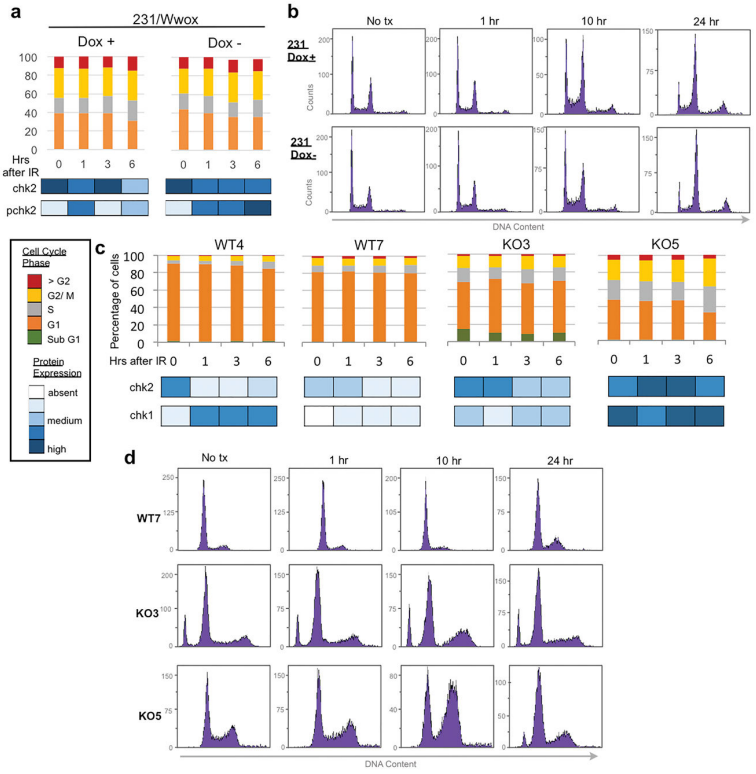

Figure 4.

Cell Cycle characterization in Wwox MEFs and 231/Wwox cells after IR. (**a**) Stacked column graph depicting cell cycle distribution of 231/Wwox cells with and without doxycycline at designated time points after 10 Gy IR. Bottom panel depicts corresponding protein expression with darker shades of blue indicating increasing intensity. (**b**) Representative images of flow cytometric DNA content analysis in 231/Wwox cells with and without doxycycline at 0, 1, 10 and 24 hrs after 10 Gy IR. (**c**) Stacked column graph depicting cell cycle distribution in wt and ko MEFs at designated time points after 10 Gy IR. Bottom panel depicts corresponding protein expression with darker shades of blue indicating increasing intensity of checkpoint proteins. (**d**) Representative flow cytometric analysis of DNA content in WT7, KO3, and KO5 at 0, 1, 10 and 24 hrs after 10 Gy IR. (**a–b**) 231/Wwox cells were untreated or induced for Wwox expression by treatment with 1 μg/ml doxycycline for 24 hrs prior to IR treatment and harvesting for flow cytometry, as described[41].

Author Manuscript Author Manuscript Author Manuscript Author Manuscript

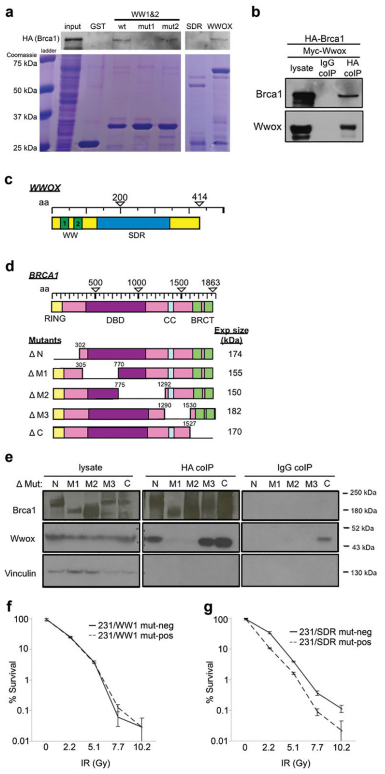

Figure 5.

Brca1 and Wwox interact in a complex through Brca1 central region. (**a**) WB and corresponding coomassie blue staining of GST pulldown using GST, and GST-Wwox WW1/WW2 fragment, GST-Wwox WW1/WW2 fragment with mutation in WW1 domain, GST-Wwox WW1/WW2 fragment with mutation in WW2 domain, GST-Wwox SDR fragment, and GST-Wwox (full-length) to IP HA-Brca1 following transfection in HEK293T cells. GST-Wwox with WW1 mutation and GST-Wwox SDR fragment do not IP HA-Brca1, suggesting that Wwox interacts with Brca1 through its first WW domain. (**b**) WB of HEK293T cells transfected with HA-Brca1 plus myc-Wwox and corresponding IPs using IgG and HA (Covance) antibodies as bait. (**c**) Schematic of Wwox domain. (**d**) Schematic of Brca1 domain and deletion mutants. (**e**) WB and corresponding HA (SCBT) coIP of MDA MB-231 cells following transfection with ΔN, ΔM1, ΔM2, ΔM3, and ΔC Brca1 deletion mutants as well as myc-Wwox. Brca1 deletion mutants are detected by polyclonal anti-Brca1[37] directed against Brca1 aa 400–1100, resulting in weaker detection of ΔM1 and ΔM2 mutants. (**f**) Graph depicting % survival of doxycycline-inducible 231 cells that express Wwox WW1 mutant with (231/WW1 mut-pos) and without (231/WW1 mut-neg) doxycycline after increasing IR doses. (**g**) Graph depicting % survival of doxycycline-inducible 231 cells that express Wwox SDR mutant with (231/SDR mut-pos) and without (231/SDR mut-neg) doxycycline after increasing IR doses.

Author Manuscript Author Manuscript Author Manuscript Author Manuscript

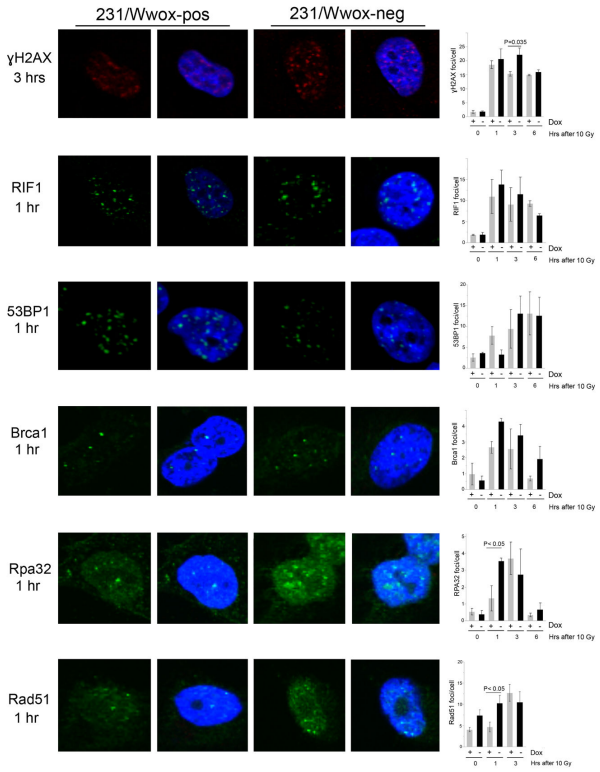

Figure 6.

Wwox significantly decreases Rpa32 and Rad51 foci formation after IR. Representative immunofluorescence images of γH2AX, RIF1, 53BP1, Brca1, Rpa32 and Rad51 foci in 231/Wwox cells untreated or treated with doxycycline (24 hours) at various time points after 10 Gy IR (left). Wwox expression significantly decreases Rpa32 and Rad51 foci 1 hour after IR and increases γH2AX foci 3 hours after IR. Graphs (right) represent protein foci averages of three independent experiments. Foci were quantified using Image J software. Experiments were performed in triplicate and statistical significance was determined using the two-tailed Student's t-test and error bars depict standard error.

Author Manuscript Author Manuscript Author Manuscript Author Manuscript

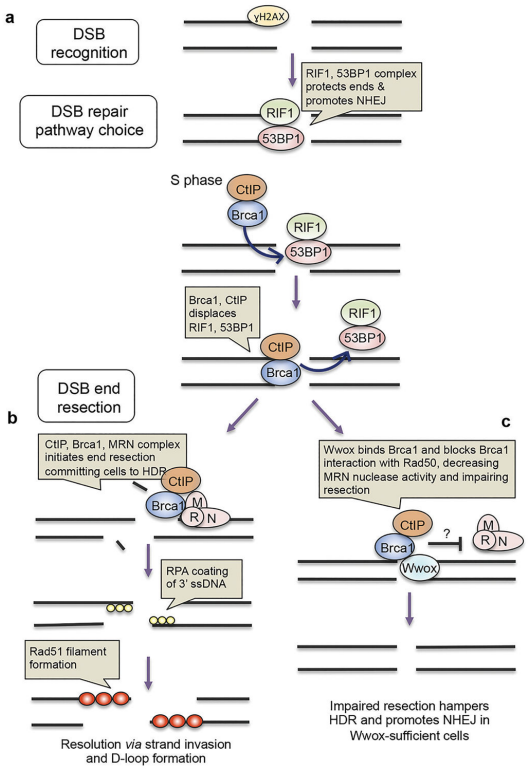

Figure 7.

IR induced foci-based hypothetical model illustrating a role for Wwox in DSB repair pathway choice. (a) γH2AX detects DSBs and recruits RIF1/53BP1 complex, which protects DSB ends. In S phase, Brca1 becomes more abundant, complexes with CtIP, displacing RIF1/ 53BP1 complex. (b) While bound to CtIP, Brca1 binds MRN complex through Rad50, stimulating nuclease activity of CtIP and MRN (complex of Mre11/Rad50/ Nbs1) resecting DNA from the 5' end. End resection commits cells to DSB repair via HDR or SSA. Following resection, RPA coats and protects 3' ss-DNA and Rad51 nucleofilament invades homologous DNA. (c) A model of putative role of Wwox in DSB repair pathway choice: in Wwox-sufficient cells, Wwox competes with Rad50 for binding to Brca1, impeding Brca1/CtIP complex binding to MRN, impairing resection. Impaired resection hampers HDR and promotes NHEJ in Wwox-sufficient cells.

Author Manuscript Author Manuscript Author Manuscript Author Manuscript

Table 1

DNA from MEFs established from two different Wwox KO mouse models[17,3] was isolated using QIAGEN DNeasy kit; DNAs of wt littermates was used in the aCGH analyses. aCGH was performed by Genome Quebec (Montreal, Canada) for genomes of Wwox +/+3/Wwox−/−5[3] and WT4/KO5[17] MEF cell line pairs. Data was filtered by removing CNVs that spanned three or fewer probes and were <0.4-fold (log2) altered *vs* wt DNA. CNVs were verified as novel by removing those associated with differences between B6/129 genomes annotated by the Mouse Genomes Project, Wellcome Trust Sanger Institute (http://www.sanger.ac.uk/resources/mouse/genomes). Losses in common between the distinct knockout mice are color-matched; Copy number losses also seen in karyotype analysis are bold; Common fragile sites are denoted by asterisk.

a. Copy Number Variations in Wwox ko MEFs[1]

Location	*Type*	*log2 value*	*Size (bp)*	*Genes*
1 C2*	loss	−1.054476	10469	
1 D	loss	−0.403978	236768	Alpi, Akp3…Efhd1, Gigyf2
1 H6	loss	−1.222192	10163	Ints7
2 A1	loss	−2.408214	148674	
2 H2 – H4	loss	−0.636356	21851075	Gm826, Mafb…Polr3k
4 B3	loss	−1.203901	20144	Klf4
4 C4 – D2.2*	loss	−0.65898	40610731	Mtap, Cdkn2a…Ccdc28b, Txlna
5 A1 – G3*	loss	−0.636989	148963374	5830415L20Rik…Vmn2r18, Rfc3
5 B3 – E2*	loss	−0.578451	55052717	Crmp1, Evc…G3bp2, Uso1
5 F – G3	loss	−0.78408	37496038	BC057022, Trpv4…Stard13, Vmn2r18
6 F3	gain	2.251792	36752	Klrb1c
6 F3	gain	2.726201	41787	Klra22, Klra15…Klra10, Klra23
7 A1 – B4	loss	−0.412604	48525504	Speer9-ps1, AU018091…Syt3
7 D1	loss	−1.025512	21457	
7 D3*	gain	3.048525	24522	
7 E3	loss	−0.954134	11544	C2cd3
7 E3*	gain	3.55613	28940	Trim12
7 E3*	gain	4.681896	27421	Gm6577
7 F1*	gain	1.63469	314615	Parva, Tead1
8 C2	loss	−0.757912	83656	Ndufb7, Tecr, Dnajb1
9 A3	loss	−2.24994	52755	Zfp872, 1810064F22Rik
9 A5.1	loss	−1.072671	93850	Thy1, Usp2…Rnf26, Mcam
12 A1.1 – A1.3	loss	−0.743706	4851016	Lpin1, Ntsr2…Adam17, Ywhaq
13 D2.2*	loss	−2.147682	62546	Fst
14 C1	gain	2.402886	199383	Ear1, Ear10, Ang3, Ang6
14 E4 – E5	gain	0.695019	8370044	Gpc5, Gpc6…Fgf14
19 C3	loss	−1.09488	10152	

Author Manuscript Author Manuscript Author Manuscript Author Manuscript

b. Copy Number Variations in Wwox ko MEFs[2]

Location	*Type*	*log2 value*	*Size (bp)*	*Genes*
1 H6	loss	−1.326041	10163	Ints7
3 A1 – H4*	loss	−0.59902	156573195	Hnf4g, Zfhx4…Rpe65, Gpr177
4 A1 – 4E2	loss	−0.422696	152029615	Lyn, Rps20…Plekhn1, Klhl17
4 E2	loss	−0.646968	2226341	Rere, Slc45a1… Kcnab2, Nphp4
6 B3	loss	−1.294899	12435	Nfe2l3
7 B1	loss	−0.429359	599038	Snx26, BC053749…Scn1b, Gramd1a
7 F3*	loss	−0887199	126255	Gsg1l
8 C2 – C3	loss	−0.469223	2732571	Zfp330, Rnf150…Orc6l, Mylk3
12 A2	gain	0.670557	2723510	Rnf144a, Rsad2, Cmpk2, Sox11, Allc
17 A1 – E5	loss	−0.475481	92128771	Rbm16, Tiam2…Adcyap1, Mettl4
18 A1*	loss	−0.50186	431578	Svil, Zfp438

[1] cell lines established frome Ludes Meyers et al, 2009 Wwox ko model

[2] cell lines established Aqeilan et al, 2008 Wwox ko model